

Higher Moment Flow Parameters From Various ADCP Transducer Configurations

Richard K. Dewey and Steve Stringer
University of Victoria
rdewey@uvic.ca and sstring@uvic.ca

The ocean contains motions on a variety of scales, both in time and space. Acoustic Doppler Current Profilers (ADCPs) can be used to measure many of these flow characteristics. The dominant modes of motion are the velocity components u , v , and w . Second are the variations of these velocities in space (shear) and time (acceleration). Although these parameters can describe much of the structure in vast regions of the ocean, even higher moments may be of interest in turbulent regions of the flow. In such dynamic regimes, the stress tensor is of vital interest. In this paper, the use of ADCPs with various transducer configurations will be reviewed with respect to measuring different components of the turbulent stress tensor. In particular, the feasibility of three, four, and five beam systems will be presented in estimating quantities such as the Reynolds Stress ($\overline{u'w'}$) and the turbulent kinetic energy ($\overline{w'^2}$). The discussion will include the benefits, short-falls, and limitations of the different beam configurations with respect to these higher moment flow parameters. Data from three, four, and five beam configurations will be presented.

1 Introduction

Acoustic Doppler current profilers are becoming the most common way that oceanographers measure currents. Whether it is from a hull mounted downward looking ADCP, or moored ADCP in an upward, horizontal, or downward profiling mode, ADCPs can remotely sample 3-dimensional flows in the water column at ranges exceeding 1000m. To accomplish this, the ADCP must have at least 3 transducers, configured such that the dominant orthogonal components of the flow are sufficiently resolved and can be extracted from the independent portions of the back-scattered signal. Although the horizontal currents U and V are often the largest and most important current components, information can be extracted on the vertical velocity, W . In coastal environments, where flows interact with topography, the vertical component can be significant, and is often similar in magnitude to the horizontal components. Such regimes are often subject to turbulent motions as well, where the velocities vary rapidly in magnitude, the structure of the flow is evolving, and the scales of the turbulent velocities are not fully resolved. Can ADCPs be used to extract additional information about these complex flows?

In this paper, we will present a summary of the analysis necessary to extract certain higher moment flow parameters from acoustic Doppler current profilers set to record data in beam coordinates, with a particular focus on the benefits and shortcomings of various transducer configurations in turbulent regimes.

Turbulent flows are, by their very nature, rather difficult to characterize. There are, however, a few terms we can use to describe turbulent environments. In a turbulent flow, the velocities vary in both space and time, at a variety of scales. In other words, the flow is inhomogeneous. It is not, however, purely random, as there is inherent structure in turbulence, which results in a certain amount of internal correlation, associated with eddies and vortices. Although the instantaneous turbulent velocities (u' , v' , and w') may be inhomogeneous, the statistical parameters of the turbulent motions (e.g. the variance of u') may vary more slowly in time and space. It is the uniform distribution of statistical parameters of turbulent flows that allows us to refer to “homogeneous turbulence” (i.e. Batchelor, 1986). One of the most important collection of such terms is the Reynolds stress tensor $\overline{u_i' u_j'}$, where the indices (i, j) are cycled from 1 to 3 and represent the orthogonal components of the flow (i.e. $u_1=u$, $u_2=v$, $u_3=w$). Thus, the Reynolds stress tensor has 9 components, although they are redundant when $i=j$. The Reynolds stress tensor is important because it tells us how forces are applied within the flow, and how momentum is transfer from one region to another. Ultimately, momentum is either gained or lost near boundaries, so the Reynolds stress allows us to understand interactions with boundary forcing, and how momentum is exchanged within the flow. It turns out, in addition to measuring the large scale mean flow parameters u , v , and w , ADCPs that record beam velocities, can be used to estimate various terms in the Reynolds stress tensor. To this end, however, not all ADCP transducer configurations provide the necessary independent information.

For this paper, we will limit the discussion to convex transducer configurations, although the same arguments and similar analysis can be performed on data collected with concave configurations. Further, although there are now ADCPs designed to project only horizontally (H-ADCP) and those with phase arrayed transducer plates (Ocean Surveyor), we will be limiting the discussion to more “standard” multi-transducer configurations that are available from a variety of providers for profiling vertically through the ocean.

2 ADCP Transducer Configurations

In order to resolve u , v , and w , at least three transducers must be configured, such that at least three components of the flow are resolved, with at least part of these components being independent between the acoustic beams. It is this independence that allows for the extraction of the orthogonal components u , v , and w . For configurations with more than three transducers (either 4 or 5), some redundant information will be available, which can be used to quantify the

“independence” of the resolved flow components. Figure 1 shows four such transducer configurations, including 3-beam, 4-beam Janus, 4-beam Cyclops, and 5-beam Janus systems.

In all of these configurations, we have fixed the vertical tilt of the transducers (those tilted away from the vertical axis of the instrument) at $\theta = 20^\circ$, although other angles (i.e. 30°) are available. Also, one of the azimuthal transducers will define the y-axis of the horizontal plane. Relative to the compass, which records heading (ϕ_1), this direction will coincide with a vector pointing north. In the 4-beam Cyclops and 5-beam Janus, the central transducer will be aligned with the central (vertical in this case) axis of the instrument. Although ADCPs are equipped with accurate pitch (ϕ_2) and roll (ϕ_3) sensors to measure the tilt about the x and y axes, respectively, for most of this paper, we will assume that the instruments are aligned such that the z axis is very nearly vertical and the compass points north, so that $\phi_1 = \phi_2 = \phi_3 \approx 0$. This is equivalent to recording in “instrument coordinates”. Heading, pitch and roll corrections are essential when the instrument is not aligned geographically or vertically, and one wishes to resolve the flow in terms the “earth” Cartesian reference frame.

The four configurations shown in Figure 1 can all generate estimates of u , v , and w under ideal conditions. These conditions typically include minimal pitch and roll, as well as minimal loss due to poor, or excessive, scattering (i.e. by fish contamination of a single beam). With 4 and 5 beam configurations, there is redundant information available if there is a beam, or, in the case of a 5 beam systems, multiple beam contamination. When calculating higher moment flow parameters, however, the redundant information can be retained to provide additional information on the nature of the flow.

To explore these higher moment flow parameters, we will need to discuss the information content of individual beams for each of the beam configurations.

3 Beam Coordinates to Velocities

An ADCP transducer sends out pulses, and receives back-scattered signals along the beam axis of the transducer. The Doppler shifted velocity is only resolved along this axis, with a positive beam velocity representing a radial flow towards the transducer face. Shown in Figure 2 are the standard definitions of various angles (azimuthal $\theta = 20^\circ$, heading ϕ_1 , pitch ϕ_2 , and roll ϕ_3) and beam numbering for the “Workhorse” 4-beam Janus configuration.

Also shown in Figure 2 is the Doppler velocity measured by beam 3 (b_3) and how, in this alignment, it resolves a combination of the horizontal velocity v (component v_3) and vertical velocity w (component w_3). With no heading, pitch, or roll correction (in an instrument reference frame), we can represent the velocities resolved by all beams of a Janus system by:

$$\begin{aligned}
b_1 &= -u_1 \sin \mathbf{q} - w_1 \cos \mathbf{q} \\
b_2 &= u_2 \sin \mathbf{q} - w_2 \cos \mathbf{q} \\
b_3 &= -v_3 \sin \mathbf{q} - w_3 \cos \mathbf{q} \\
b_4 &= v_4 \sin \mathbf{q} - w_4 \cos \mathbf{q} \\
b_5 &= -w_5
\end{aligned} \tag{3.1}$$

where a standard 4-beam Janus would record only beams 1 through 4, and the 5-beam Janus would include the fifth vertical beam b_5 . We note that for beams 1 – 4, each beam has resolved at least two orthogonal velocity components. For example, the horizontal component resolved by beams 1 and 2, namely, u_1 and u_2 are both representing the “same” u component of horizontal velocity, and all four beams are seen to resolve some fraction of the vertical velocity w . If the flow is homogeneous (spatially uniform), then there is no spatial variations in the flow between beam estimates of the primary flow velocities, which can then be combined following:

$$\begin{aligned}
u_{12} &= (b_2 - b_1) / 2 = ([u_2 + u_1] \sin \mathbf{q} + [w_1 - w_2] \cos \mathbf{q}) / 2 \\
v_{34} &= (b_4 - b_3) / 2 = ([v_4 + v_3] \sin \mathbf{q} + [w_3 - w_4] \cos \mathbf{q}) / 2 \\
w_{12} &= -(b_1 + b_2) / 2 = ([w_1 + w_2] \cos \mathbf{q} + [u_1 - u_2] \sin \mathbf{q}) / 2 \\
w_{34} &= -(b_3 + b_4) / 2 = ([w_3 + w_4] \cos \mathbf{q} + [v_3 - v_4] \sin \mathbf{q}) / 2
\end{aligned} \tag{3.2}$$

where the primary flow velocities are then given by $u = u_{12}$, $v = v_{34}$, and $w = (w_{12} + w_{34}) / 2$. This inversion is identical to applying the “**instrument transformation matrix**” as described in RDI’s Technical Manuals. We note that the assumption of homogeneity assumes $u_1 = u_2$ and $v_3 = v_4$, and $w_1 = w_2$ and $w_3 = w_4$. In many high Reynolds number, or turbulent flows, this requirement of homogeneity may be a poor assumption. More on that shortly.

The 3-beam and 4-beam Cyclops systems also record beam velocities that can be mapped to u , v , and w with a similar set of equations:

$$\begin{aligned}
b_1 &= v_1 \sin \mathbf{q} - w_1 \cos \mathbf{q} \\
b_2 &= u_2 \sin \mathbf{q} \sin \frac{\mathbf{p}}{3} - v_2 \sin \mathbf{q} \cos \frac{\mathbf{p}}{3} - w_2 \cos \mathbf{q} \\
b_3 &= -u_3 \sin \mathbf{q} \sin \frac{\mathbf{p}}{3} - v_3 \sin \mathbf{q} \cos \frac{\mathbf{p}}{3} - w_3 \cos \mathbf{q} \\
b_4 &= -w_4
\end{aligned} \tag{3.3}$$

where only the 4-beam Cyclops system includes the beam 4 estimate of w_4 , and beam 1 is assumed to be aligned with the compass ($\phi_1 = \pi$). In a similar manner, under the assumption of homogeneity, equations (3.3) can be inverted to provide estimates for the velocities u_{123} , v_{123} , w_{123} , v_{14} , w_{123} , w_{1234} , and w_4 , where we have noted the dependence on the beam measurement in the subscripts and only the 4-beam Cyclops generates any velocity estimates with subscript 4. For these transducer configurations (3-beam, or 4-beam Cyclops), at least three of the beam velocities contain contributions from *all* three orthogonal Cartesian velocity components, and since all beams resolve some fraction of w , a vertical velocity estimate can be obtained by combining all

beams (thus w_{1234}). This inter-dependence will, however, prove costly when analyzing the beam velocities for stresses estimates. It should be noted that for all transducer configurations the formulae become significantly more complicated, and the velocity estimates even more inter-dependent when the pitch and/or roll angles are non-zero. It is beyond the scope of this paper to present these more complete inversions, although small angle versions will be discussed in section 6.

In estimating the “standard” Cartesian velocities u , v , and w , [i.e. equations (3.2)], the flow is assumed to be homogeneous. A measure of the inhomogeneity is returned by the ADCP (or WinADCP) as the “error” velocity, $e = w_{12} - w_{34}$. If the flow is inhomogeneous, then the two independent estimates of w (w_{12} and w_{34}) are likely to be different. The larger the difference, the larger the error velocity, and the more inhomogeneous the flow. If the error velocity is large, and the flow is inhomogeneous, it is just as likely that horizontal velocities from the different beams are non-equal, namely $u_1 \neq u_2$, and $v_3 \neq v_4$. Differences in the horizontal velocities have the potential of being large (certainly larger than differences in w). By assuming homogeneity, these velocity differences (errors) are automatically mapped into all velocity estimates (u , v , and w). So a large error velocity does not just represent an uncertainty in w , but represents an increased uncertainty in all velocity estimates. Fortunately, in many oceanic flows, u and v are likely to be larger than w , and their relative uncertainty may remain small. Relative, and absolute confidence in w , however, may be significantly compromised within inhomogeneous flows. It is for this reason, that vertical beam ADCPs are of interest in turbulent and variable flow environments.

4 Inhomogeneous and Turbulent Flows

In this paper, we are interested in variable and turbulent flows, and should therefore ask: What additional information is in the ADCP data collected in a turbulent or inhomogeneous flow? If the flow is turbulent and inhomogeneous, then the assumptions leading to the transformation from beam coordinates to “earth” velocities, as given by equations (3.2), are in slight error. In particular $u_1 \neq u_2$, $v_3 \neq v_4$, and $w_1 \neq w_2$ and $w_3 \neq w_4$. Similar inequalities exist for the 3-beam and 4-beam Cyclops transformations. So our first lesson is that ADCP measurements have higher uncertainty when the flow is turbulent, or at least variable on the scales of the separation of the beams. But it is this very inhomogeneity that contains information on the nature of the turbulence. So our goal is to capitalize on this problem, and turn it into a benefit.

Much research on the nature of turbulence has taught us that although the instantaneous velocities are rather chaotic, the statistics and structure of the chaos can be enlightening, even with regard to very important turbulent parameters, namely, the Reynolds stress tensor, and the rate of dissipation of turbulent kinetic energy, ϵ . In many turbulent flows, especially those found in nature, where the Reynolds Number is large, the Eulerian (fixed in space as opposed to moving with the flow) statistics can be rather stable in time, and often homogeneous in space. Let us now

explore the information contained in the beam velocities that is related to some higher moment flow parameters.

The Reynolds stress tensor per unit mass $-\overline{u_i' u_j'}$ is formally given by

$$\begin{bmatrix} -\overline{u'u'} & -\overline{u'v'} & -\overline{u'w'} \\ -\overline{u'v'} & -\overline{v'v'} & -\overline{v'w'} \\ -\overline{u'w'} & -\overline{v'w'} & -\overline{w'w'} \end{bmatrix} \quad (4.4)$$

where the velocity symbols have been primed to indicate they are the “fluctuating” part of the flow, and are to be distinguished from the “mean” large scale flow velocities by the Reynolds decomposition, $u = \bar{u} + u'$. In this, and subsequent discussion, the over-bar symbol will denote an average quantity. For our analysis, an average will be determined temporally, by considering some averaging interval over which the external forcing (e.g. tides) is constant.

There are two different components of the Reynolds stress tensor that need to be further identified. First are the diagonal terms, such as $\overline{u'u'}$. These terms represent the turbulent kinetic energy in the three components of the flow in the Cartesian coordinates x , y , and z , summed they are the total turbulent kinetic energy (TKE). The off-diagonal terms, such as $\overline{u'w'}$, represent turbulent momentum fluxes, and are only significant (non-zero) if the turbulence is anisotropic (i.e. there is a preferential direction to the turbulent flux of momentum). The product $\overline{u'w'}$ can be thought of as the vertical flux (w') of the x momentum deficit (u'). These stress terms reflect the transport of momentum within the flow, either towards or away from boundaries, and within the flow across shear or strain zones. They are fundamental in terms of both the mean and turbulent dynamics of the flow. Understanding them is paramount to understanding complex and evolving flows. Even fluid dynamic models must estimate the internal stresses, where they are often parameterized in terms of eddy diffusivities. Measuring them is difficult, but recently ADCPs have been used to quantify important Reynolds stress components (Lohrmann *et al*, 1990; Lu and Lueck, 1999; Rippeth *et al*, 2002).

5 Beam Velocities to Reynolds Stress

If the statistical properties of the turbulence are spatially homogeneous, then $\overline{u_i'^2} = \overline{u_j'^2} = \overline{u'^2}$, where i and j are any two independent beam indices. A similar assumption can be made for the v' and w' components of a homogeneous turbulent flow. For a standard 4-beam Janus system, with orthogonal pairs of transducer planes (Figure 1b), the beam variances are:

$$\begin{aligned}
\overline{b_1'^2} &= \overline{u_1'^2} \sin^2 \mathbf{q} + \overline{w_1'^2} \cos^2 \mathbf{q} + 2\overline{u_1'w_1'} \sin \mathbf{q} \cos \mathbf{q} \\
\overline{b_2'^2} &= \overline{u_2'^2} \sin^2 \mathbf{q} + \overline{w_2'^2} \cos^2 \mathbf{q} - 2\overline{u_2'w_2'} \sin \mathbf{q} \cos \mathbf{q} \\
\overline{b_3'^2} &= \overline{v_3'^2} \sin^2 \mathbf{q} + \overline{w_3'^2} \cos^2 \mathbf{q} + 2\overline{v_3'w_3'} \sin \mathbf{q} \cos \mathbf{q} \\
\overline{b_4'^2} &= \overline{v_4'^2} \sin^2 \mathbf{q} + \overline{w_4'^2} \cos^2 \mathbf{q} - 2\overline{v_4'w_4'} \sin \mathbf{q} \cos \mathbf{q}
\end{aligned} \tag{5.5}$$

Subtraction of the beam pairs 1 and 2, and 3 and 4, and assuming that the turbulence is homogeneous, such that $\overline{u_1'^2} \square \overline{u_2'^2}$, $\overline{v_3'^2} \square \overline{v_4'^2}$, and $\overline{w_1'^2} \square \overline{w_2'^2}$, $\overline{w_3'^2} \square \overline{w_4'^2}$ leads to,

$$\begin{aligned}
-\overline{u'w'} &= \frac{1}{2\sin 2\mathbf{q}} \left(\overline{b_2'^2} - \overline{b_1'^2} \right) \\
-\overline{v'w'} &= \frac{1}{2\sin 2\mathbf{q}} \left(\overline{b_4'^2} - \overline{b_3'^2} \right)
\end{aligned} \tag{5.6}$$

which is valid for zero pitch and roll under the assumption of homogenous turbulence. This is possible because the 4 transducers resolve independent components that are orthogonal in two planes, and the beam variances are much more likely to be homogeneous than the beam velocities. The requirement is that the statistics of the turbulence be homogeneous, even if the instantaneous velocities are not. These two orthogonal stress estimates are important components of the Reynolds stress tensor in the ocean, as they represent the vertical flux of horizontal momentum variation. As an example, both wind and bottom stresses are communicated into the fluid through these key terms.

The 3-beam (Figure 1a) transducer configuration produces no independent stress estimates when the beam variances are combined. When the 4-beam Cyclops system is considered, with a direct measurement of w' , and therefore $\overline{w'^2}$, the beam variances combine to produce,

$$\begin{aligned}
-\overline{u'w'} &= -\frac{1}{2\sin 2\mathbf{q} \sin \frac{\mathbf{p}}{3}} \left(\overline{b_3'^2} - \overline{b_2'^2} \right) + \frac{1}{2} \tan \mathbf{q} \overline{u'v'} \\
-\overline{v'w'} &= \frac{1}{2\sin 2\mathbf{q}} \left(\overline{b_1'^2} - \cos 2\mathbf{q} \overline{b_4'^2} \right) - \frac{1}{2} \tan \mathbf{q} \overline{v'^2} \\
\left(\overline{u'^2} + \overline{v'^2} \right) &= \frac{2}{3\sin^2 \mathbf{q}} \left[\overline{b_1'^2} + \overline{b_2'^2} + \overline{b_3'^2} - 3\cos^2 \mathbf{q} \overline{b_4'^2} \right] \\
\overline{w'^2} &= \overline{b_4'^2}
\end{aligned} \tag{5.7}$$

where the Reynolds stress terms $-\overline{u'w'}$ and $-\overline{v'w'}$ are seen to have contamination cross-talk from the dependent beam information (i.e. $\overline{u'v'}$). Equations (5.7) do, however, reveal two important quantities with only independent beam variance terms. These are the horizontal

turbulent kinetic energy $\left(\overline{u'^2} + \overline{v'^2}\right)$ and the vertical turbulent kinetic energy $\overline{w'^2}$, which, when added are the total TKE. Further, if the horizontal components of the turbulence (u' and v') are isotropic (i.e. insensitive to coordinate rotations, $\overline{u'v'} = 0$, Figure 3) and the vertical fluctuations are small compared to the horizontal fluctuations $\overline{w'^2} \ll \left(\overline{u'^2}, \overline{v'^2}\right)$, then the Cyclops configuration of beam variances can be re-arranged to obtain:

$$\begin{aligned} -\overline{u'w'} &= -\frac{1}{2\sin 2\mathbf{q} \sin \frac{\mathbf{p}}{3}} (\overline{b'_3} - \overline{b'_2}) \\ -\overline{v'w'} &= -\frac{1}{6\sin 2\mathbf{q}} \left[2(\overline{b'_3} - \overline{b'_2}) - (\overline{b'_1} - 3\overline{b'_4}) \right] \end{aligned} \quad (5.8)$$

These necessary flow and isotropy requirements can be met. It does not require that u' or v' be zero, only that they are uncorrelated, and the mean stress $\overline{u'v'} = 0$ (Figure 3). This could occur far from any side-wall effect or lateral boundary, which would tend to introduce a bias in the direction of the horizontal stress. Similarly, in many stratified ocean flows, $u > w$, and often $u' > w'$. If the turbulent flow is horizontally isotropic, and this can be tested by plotting u' against v' , then a vertically oriented Cyclops configuration provides a slightly contaminated estimate of the vertical Reynolds stress, but insight into the turbulent kinetic energy. Once again, we have stipulated that the ADCP be nearly identically aligned in the vertical orientation. Tilts greater than approximately $4-5^\circ$ will begin to introduce significant inter-beam dependences that cannot be removed through combinations of the beam variances.

Finally, let us consider the 5-beam Janus configuration. Here we have the standard four Janus beams aligned into two orthogonal planes and a vertical beam, as indicated in equations (3.1). The first four beam variances can be combined to give the vertical Reynolds stress terms (5.6), and the vertical beam provides a direct, and independent estimate of $\overline{w'^2}$. With this information, we can introduce a new parameter, the anisotropy ratio \mathbf{a} , which is the ratio of the vertical to horizontal turbulent kinetic energy:

$$\begin{aligned} \mathbf{a} &= \frac{\overline{w'^2}}{\overline{u'^2} + \overline{v'^2}} = \frac{2\sin^2 \mathbf{q} \overline{b'_5'^2}}{\overline{b'_1'^2} + \overline{b'_2'^2} + \overline{b'_3'^2} + \overline{b'_4'^2} - 4\cos^2 \mathbf{q} \overline{b'_5'^2}} \\ q^2 &= \overline{u'^2} + \overline{v'^2} + \overline{w'^2} = \frac{\overline{b'_1'^2} + \overline{b'_2'^2} + \overline{b'_3'^2} + \overline{b'_4'^2} - 4\cos^2 \mathbf{q} \overline{b'_5'^2} + 2\sin^2 \mathbf{q} \overline{b'_5'^2}}{2\sin^2 \mathbf{q}} \end{aligned} \quad (5.9)$$

and q^2 , which represents the total turbulent kinetic energy (TKE). The anisotropy ratio, \mathbf{a} , is an indicator of the partition of energy between the vertical and horizontal components of the turbulence. In stratified ocean environments, one often finds that the vertical velocities are

suppressed by the work they do against buoyancy forces, and the turbulence can become “flattened” and anisotropic.

6 Data Analysis

Within the scope of this paper, we will present some preliminary results from our data analysis that includes data representing all four transducer configurations shown in Figure 1. The data were collected in Sansum Narrows, between Vancouver Island and Saltspring Island (Figure 4). The channel is known for its vigorous tides, which can exceed 4 knots, and the active mixing of stratified coastal waters (Macoun, 2002). Two ADCPs (a 4-beam Cyclops Figure 5, and a 4-beam Janus) were deployed for a week in August 2000, and a 5-beam Janus configuration (Figure 6) was deployed for two weeks in January 2003. The two bottom mounted ADCPs deployed in 2000 had a spatial separation of only 120m in water 80 m deep, and were set to sample 16 ping ensembles every 10 seconds. The 5-beam Janus ADCP was deployed in 60 m of water slightly north-west of the dual moorings of 2000 (Figure 4), and consisted of two 4-beam Janus ADCPs coupled in a Master-Slave mode, with one permanently tilted at 20 degrees relative to the vertical so that one of its beams was pointed identically vertical (Figure 6). The 5-beam configuration ended up recording 5 ping ensembles every 6.6 seconds. All instruments were programmed to record 1 m bins in beam coordinates.

For the Janus and Cyclops ADCPs deployed in 2000, each was mounted in a gimballed bracket. Despite every effort to get both aligned with minimal pitch and roll, the Janus ADCP ended up landing with a rather significant tilt (roll \approx -4 $^\circ$, pitch \approx -7.5 $^\circ$). The Cyclops, with its vertical beam, settled with a roll of only 0.7 $^\circ$ and a pitch that slowly increased from 0.8 $^\circ$ to 1.1 $^\circ$. The significant tilt in the 4-beam Janus configuration was less than ideal, and caused slight contamination of the estimates of the vertical velocity during peak tidal flow. Additionally, bin mapping was required in order to match appropriate depths for different beams. In the 2003 data, the 5-beam Janus configuration was mounted so the ADCPs were more rigid in the bracket, as to retain the alignment of the vertical beam of the tilted ADCP with the vertical 4-beam Janus. None-the-less, the bottom bracket landed on a slight slope and all transducers were tilted from their vertical alignment by nearly 5 $^\circ$. Consequently, the following analysis includes slight corrections for the observed pitch and roll, not included in the simplified equations presented above.

Our raw data, although recorded in beam coordinates, includes contributions from the mean flow and the turbulent fluctuations, $u = \overline{u} + u'$. To perform a “Reynolds decomposition”, we must determine two time intervals from which we can estimate Reynolds stresses. First is the time interval over which the mean flow is reasonably stable (constant). The second is the time interval over which we will estimate our beam variances. The flow in Sansum Narrows is dominated by a semi-diurnal tide. To estimate the slowly varying “mean” flow, we have used a

20 minute filter. The residual obtained by subtracting the original beam velocities from the filtered data provides an estimate of the “fluctuating” part of the flow, i.e. b' (e.g. Figure 7a). From these residual beam velocities, we can estimate beam variances and Reynolds stresses. Based on the power spectrum, beam variances over intervals of 2, 4 and 6 minutes were examined, with a slight decrease in the variances with a longer interval (e.g. Figure 7b). Subsequent analysis uses 2 minute (~12 ensemble) averages to obtain beam variances and the related Reynolds stresses.

Due to the relatively large pitch and roll angles recorded by the 4-beam Janus ADCP in August 2000, we will need to introduce the corrections to (5.6) associated with the bias from the tilted beams, namely:

$$\begin{aligned} -\overline{u'w'} &\square \frac{1}{2\sin 2\mathbf{q}} \left(\overline{b_2'^2} - \overline{b_1'^2} \right) + \frac{\mathbf{f}_3}{\sin^2 \mathbf{q}} \left[\frac{1}{2} \left(\overline{b_1'^2} + \overline{b_2'^2} \right) - \overline{w'^2} \right] - \mathbf{f}_2 \overline{u'v'} \\ -\overline{v'w'} &\square \frac{1}{2\sin 2\mathbf{q}} \left(\overline{b_4'^2} - \overline{b_3'^2} \right) + \frac{\mathbf{f}_2}{\sin^2 \mathbf{q}} \left[\frac{1}{2} \left(\overline{b_3'^2} + \overline{b_4'^2} \right) - \cos 2\mathbf{q} \overline{w'^2} \right] - \mathbf{f}_3 \overline{u'v'} \end{aligned} \quad (6.10)$$

where the pitch (\mathbf{f}_2) and roll (\mathbf{f}_3) are still assumed to be small, so that the small angle approximation ($\sin\phi \cong \phi$ in radians, and $\cos\phi \cong 1$) can be made. The differences between (5.6) and (6.10) will be referred to as the tilt biases caused by contamination of each beam velocity with some contribution from each of u , v , and w flow components.

Shown in Figures 8 are the 2 minute Reynolds stress estimates (blue) for a) $-\overline{u'w'}$ and b) $-\overline{v'w'}$ from the 4-beam Janus ADCP (August 2000 deployment). The units of the Reynolds stress terms are m^2s^{-2} . Also shown (red and green) are the small-angle bias contributions associated with non-zero pitch and roll angles included in equation (6.10) for a 4-beam Janus configuration. There are a number of features worth pointing out in these data. First, for pitch and roll angles of the order 5° , the bias terms (red and green) arising from the tilted beams can be of similar magnitude to the stress terms represented by the beam variances alone. However, for most of the records, these bias terms are small. Another common feature of Reynolds stresses is the intermittent nature of the stresses, even in a vigorously turbulent tidal channel. Large Reynolds stresses tend to be relatively short-lived, high-correlation events, occurring at specific periods during the tidal flow (Figure 7). Finally, for a specific location, either vertically or horizontally, one typically finds that for a particular Reynolds stress term, it frequently has a bias towards one sign. This too is encouraging, as one might expect to find a bias in the momentum flux at a particular location in a flow (e.g. flux of momentum away from, or towards, a boundary region). The 4-beam Janus, however, can not estimate the turbulent kinetic energy. To obtain this, we will to explore the data generated by vertical beam ADCPs, either the 4-beam Cyclops or 5-beam Janus configurations.

First, let us view some 4-beam Cyclops data collected in conjunction with the 4-beam Janus data shown in Figures 7 and 8. We know that the vertical beam of the Cyclops will give us a direct estimate of $\overline{w'^2}$, but what about the vertical Reynolds stress terms $-\overline{u'w'}$ and $-\overline{v'w'}$. Even though the Cyclops ADCP was deployed with relatively small ($<1^\circ$) pitch and roll angles, it will be useful to see the full algebraic expressions for these stress terms assuming the small angle approximation, names;

$$\begin{aligned}
-\overline{u'w'} & \square \frac{1}{\sin 2\mathbf{q} \sin \frac{\mathbf{p}}{3} (2\cos \mathbf{q} - 3\mathbf{f}_2 \sin \mathbf{q})} \left\{ (2\mathbf{f}_2 \sin \mathbf{q} - \cos \mathbf{q}) (\overline{b_3'^2} - \overline{b_2'^2}) \right. \\
& + \mathbf{f}_3 \sin \mathbf{q} \sin \frac{\mathbf{p}}{3} (\overline{b_1'^2} - \overline{b_4'^2}) + 4\mathbf{f}_3 \sin \mathbf{q} \cos^2 \mathbf{q} \sin \frac{\mathbf{p}}{3} (\overline{u'^2} - \overline{w'^2}) \\
& \left. - \mathbf{f}_3 \sin^3 \mathbf{q} \sin \frac{\mathbf{p}}{3} (\overline{v'^2} - \overline{w'^2}) + 2\sin \mathbf{q} \sin \frac{\mathbf{p}}{3} (\sin \mathbf{q} \cos \mathbf{q} - 2\mathbf{f}_2) \overline{u'v'} \right\} \\
-\overline{v'w'} & \square \frac{1}{\sin 2\mathbf{q} \sin \frac{\mathbf{p}}{3} (2\cos \mathbf{q} - 3\mathbf{f}_2 \sin \mathbf{q})} \left\{ (2\cos \mathbf{q} + \mathbf{f}_2 \sin \mathbf{q}) \sin \frac{\mathbf{p}}{3} (\overline{b_1'^2} - \overline{b_4'^2}) \right. \\
& + \mathbf{f}_3 \sin \mathbf{q} (\overline{b_3'^2} - \overline{b_2'^2}) - \sin \mathbf{q} \sin \frac{\mathbf{p}}{3} \left[\sin 2\mathbf{q} + \mathbf{f}_2 (4\cos^2 \mathbf{q} + \sin^2 \mathbf{q}) \right] (\overline{v'^2} - \overline{w'^2}) \\
& \left. + 2\mathbf{f}_3 \sin^2 \mathbf{q} \sin \frac{\mathbf{p}}{3} (2\cos \mathbf{q} + \sin \mathbf{q}) \overline{u'v'} \right\}
\end{aligned} \tag{6.11}$$

These equations will allow us to determine were biases from the azimuthal beams and non-zero pitch and roll terms will contaminate the Reynolds stress estimates. In general, terms that are directly multiplied by the pitch and roll angles using the small angle approximation, will be relatively small. Examination of (6.11) reveals that in both stress terms, there are contributions from biases not subject to this minimization. Figure 9 shows the Reynolds stresses from data collected with the 4-beam Cyclops deployed in August 2000, and the contributions from the more significant bias terms in (6.11). Among the differences between Figures 8 and 9, several key features are worth pointing out. First off, we note that periods of higher stress occur at similar times in both records. Secondly, the estimates of $-\overline{u'w'}$ from the vertical beam Cyclops (Figure 9a) are significantly larger than those obtained from the 4-beam Janus (Figure 8a). This is due to the direct contribution of the vertical beam variance to the stress, which resolves the finer structures in the flow (this will be elaborated on below). Finally, the $-\overline{v'w'}$ stress estimate from the 4-beam Cyclops reveals the most pressing limitation on this configuration. Figure 9b shows that the stress estimate is dominated by contributions coming from the $\overline{v'^2}$ component, which is

not subject to multiplication by the pitch or roll angles. In other words, despite resolving the vertical velocity directly, the 3 azimuthal beams of the Cyclops cannot resolve orthogonal components of the stress without serious contamination leaking in from the dependent measurements of the horizontal flow. Consequently, the 4-beam Cyclops can reasonably measure stress in two of the three orthogonal coordinates, but not all three. If one were able to align the Cyclops in a preferred axis of the flow, this short-coming could be reduced, but often it is this very axial orientation to the stress field which is of most interest.

Finally, we will have a brief and preliminary examination of data collected with a 5-beam Janus configuration. This data was collected in January 2003, only a month before this presentation, and as such, the full Reynolds stress analysis has not been completed. Several features of this deployment are, however, worth discussing. First off, a 5-beam Janus as depicted in Figure 1 was not used, but a “poor-mans” version was configured using two 4-beam Janus ADCPs coupled together using a Master-Slave cable (Figure 6). The Master ADCP was aligned vertically, and told to send a sync pulse to the Slave ADCP preceding each ping. The Slave ADCP was mounted with a 20° tilt, such that beam 3 was pointing vertically. The Slave was then programmed to ping 400ms after receiving the sync pulse from the Master. Thus the two ADCPs alternated pings, approximately once per second, recording synchronized 5 ping ensembles in beam coordinates every 6.64 seconds.

Shown in Figure 10 is the first full 24 hours of mean u , v , and w data from Sansum Narrows, as resolved by the Master ADCP. The semi-diurnal nature of the tides is evident, with peak tidal velocities exceeding 1 m/s. Shown in Figure 11 are one hour sections of vertical velocity data straddling mid-night on the first day. The panels, from top to bottom represent, a) the vertical velocity as recorded by the vertical beam from the Slave ADCP, b) the vertical velocity from beam pairs 1 & 2 from the Master, c) the vertical velocity from beams 3 & 4 from the Master, and d) the error velocity from the Master, the difference between panels b) and c).

Several features are worth identifying. First, there are a number of periods when there are vigorous vertical velocities associated with turbulent eddies within Sansum Narrows in all panels. Often these vertical velocities have short time scales associated with them (i.e. near 23:40), a result of either fine scale structure in the turbulence or a strong advection effect in the tidal flow, and at other times the structures in the flow are larger and longer lived (i.e. 00:15). Let us examine differences between the vertical beam w_v , and the standard Janus estimated w from the beam pairs 1&2 (w_{12}) and 3&4 (w_{34}). Between 23:40 and 23:50, all three estimates reveal fine resolution turbulent structures. Some of these structures are resolved to a similar extent, while others are not. This is due to inhomogeneities in the turbulence. If beams 1 & 2 see a different flow in u or w , then these differences are mapped into the estimates of both u_{12} and w_{12} . Similarly, if beams 3 & 4 see different flows, then these differences are mapped into the estimates of both v_{34} and w_{34} . In a turbulent flow, there is often deformation on the scale of the

beam separation, and the resulting discrepancy between velocities gives rise to errors in u , v , and w , as well as the Reynolds stress estimates. It is worth noting that this error grows with distance from the ADCP head, as the beam separation grows. Typically, there is no way to know which velocity component (either u , v , or w , or combination) is different between the beams, only that by examining the error velocity, we can see that w_{12} and w_{34} are often quite different. This would imply that the vertical velocity across the beam pairs might be different, but in actuality, the error velocity could be representing inhomogeneity in any of the velocity components. It is these differences in the estimates of a single velocity estimate that give rise to “contamination” in the dependent estimates of Reynolds stress as determined using equations (6.10) and (6.11).

With the dedicated vertical beam, however, we can identify whether the inhomogeneity is in both, or only one of the beam planes. At times, the vertical velocity resolved by the beam pairs [panels b) and c)] closely resemble the vertical velocities resolved by the single vertical beam, both in scale and magnitude (i.e. near 00:00 - 00:15, Figure 11). When all three estimates of w reveal a common structure, we would have confidence in a number of quantities. Such patterns usually have broader time scales (i.e. tens of minutes), which would correspond to larger spatial scales and support the contention that all 5 beams are “seeing” the same flow. This goes for both the directly resolved vertical velocity w , as well as the horizontal components, which are obtained by subtracting beam velocities in a plane. Further, if the flow is more homogeneous, then the Reynolds stress estimates, which include both beam variance differences, and terms involving velocity variances and co-variances, will also likely combine in a more coherent way when estimating the stresses given in (6.10) and (6.11).

7 Conclusions

Acoustic Doppler current profilers have become common tools for measuring ocean currents. Two typical transducer configurations, a 3-beam symmetric and 4-beam Janus, both provide accurate measurements of the orthogonal mean flow velocities u , v , and w . However, when using raw beam velocities to estimate higher moment flow parameters, such as the Reynolds stresses and turbulent kinetic energy, there are significant differences between these two configurations (Table 1). Generally, the 4-beam Janus, with its transducer pairs in orthogonal planes, provides a means of estimating the $-\overline{u'w'}$ and $-\overline{v'w'}$ Reynolds stress terms under the assumption of homogeneous turbulence. With the addition of a dedicated vertical beam to these standard transducer configurations, we have examined the preliminary benefits and shortcomings of both the 4-beam Cyclops and 5-beam Janus systems. In general, the addition of a vertical beam allows the direct estimation of the vertical component of the turbulent kinetic energy. Further, it allows an independent assessment of the homogeneity of the flow, and therefore can be analyzed to determine when, and if the flow meets the necessary assumptions to

apply confidence in u , v , and w , as well as the Reynolds stress and the horizontal turbulent kinetic energy estimates.

Table 1. Various measurable quantities for different transducer configurations, with assumptions and limitations.

	U, V, W		$-\overline{u'w'}$ and $-\overline{v'w'}$		$\overline{u'^2}, \overline{v'^2}, \overline{w'^2}$	
		Assumptions		Assumptions		Assumptions
3 Beam	Yes	No Redundancy	No	Insufficient Information	No	Insufficient Information
4 Beam Cyclops	Yes	With some Redundancy	Yes	Parital, only One.	$\overline{w'^2}$ only	Only Vertical
4 Beam Janus	Yes	With Redundancy	Yes	Homogeneous Turbulence	No	Insufficient Information
5 Beam Janus	Yes	With Redundancy	Yes	Homogeneous Turbulence	Yes	Isotropic Turbulence

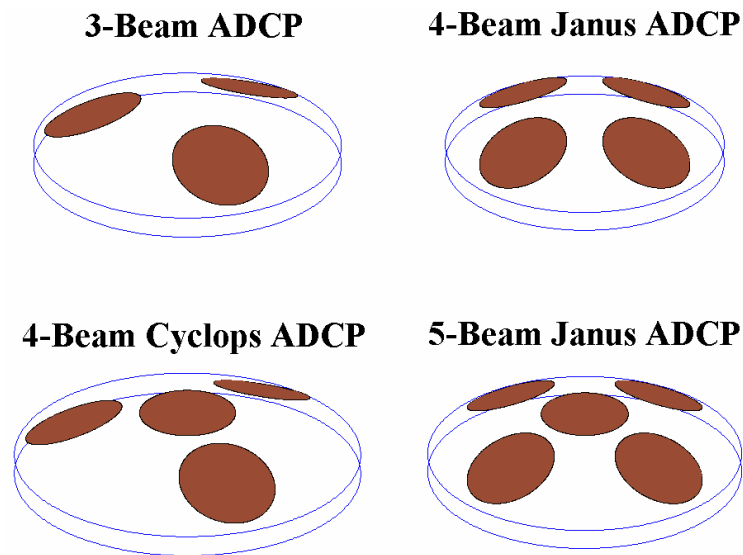


Figure 1. Various ADCP configurations: 3-beam (a), 4-beam Janus (b), 4-beam Cyclops (c), and 5-beam Janus (d), all in an upward pointing orientation.

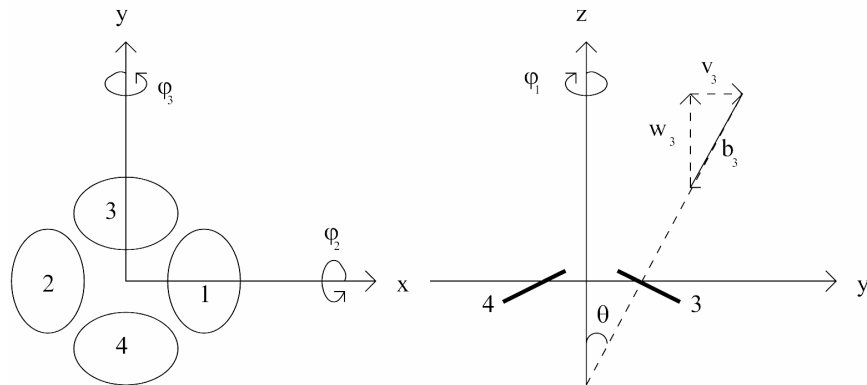


Figure 2. Beam numbering, Heading (j_1), Pitch (j_2), Roll (j_3), and azimuthal angle (q) for a standard “Workhorse” 4-beam Janus ADCP.

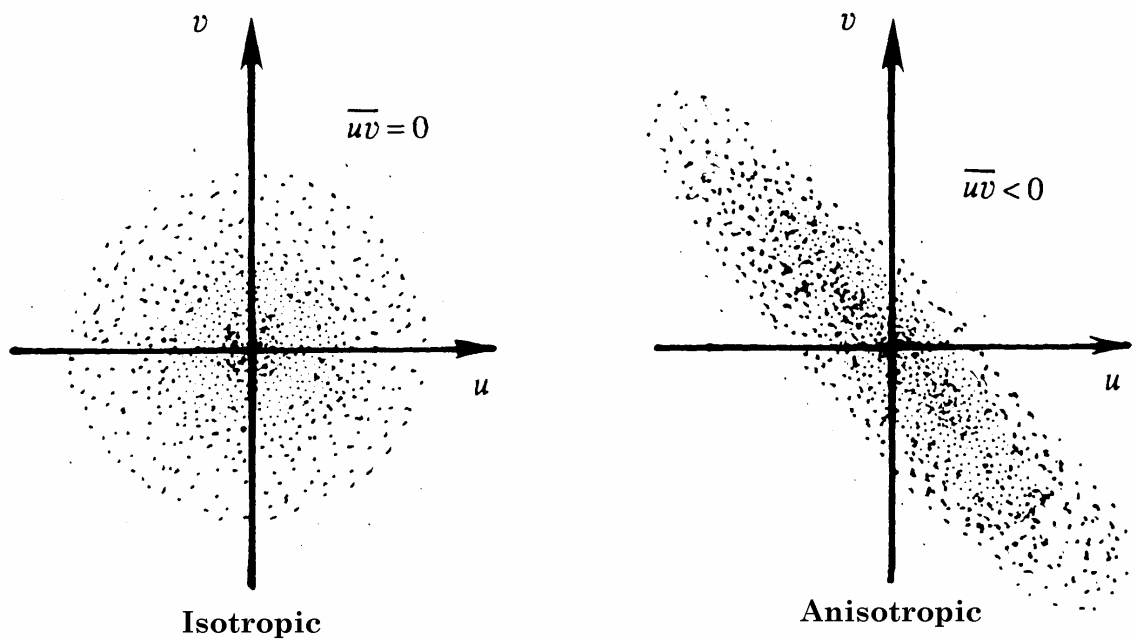


Figure 3. Horizontal stress in either an isotropic or anisotropic turbulent flow. Only the anisotropic flow has a net stress.

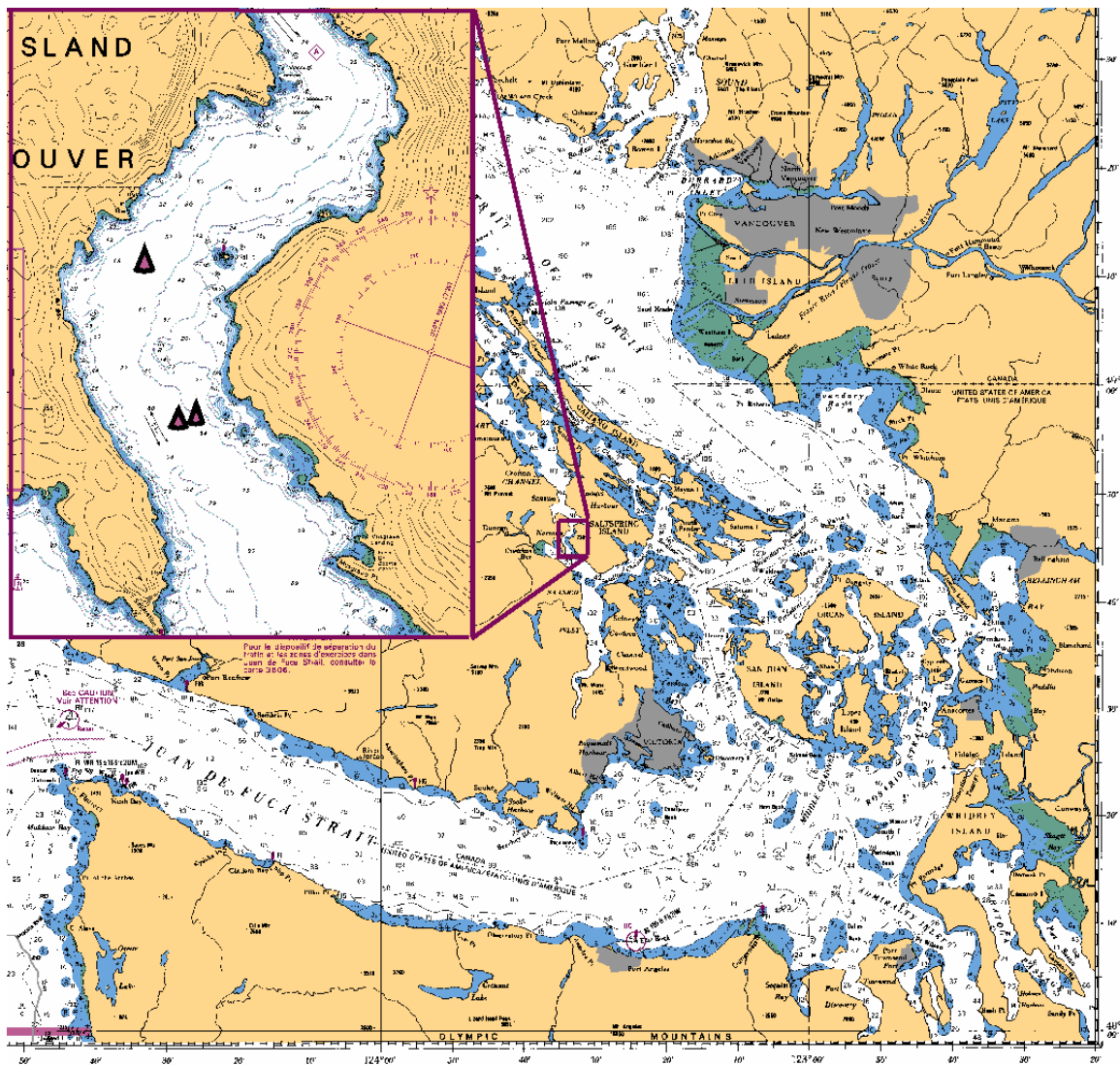


Figure 4. The tidal channel of Sansum Narrows, between Vancouver Island and Saltspring Island, where 4-beam Janus, 4-beam Cyclops, and 5-beam Janus ADCP configurations were deployed.

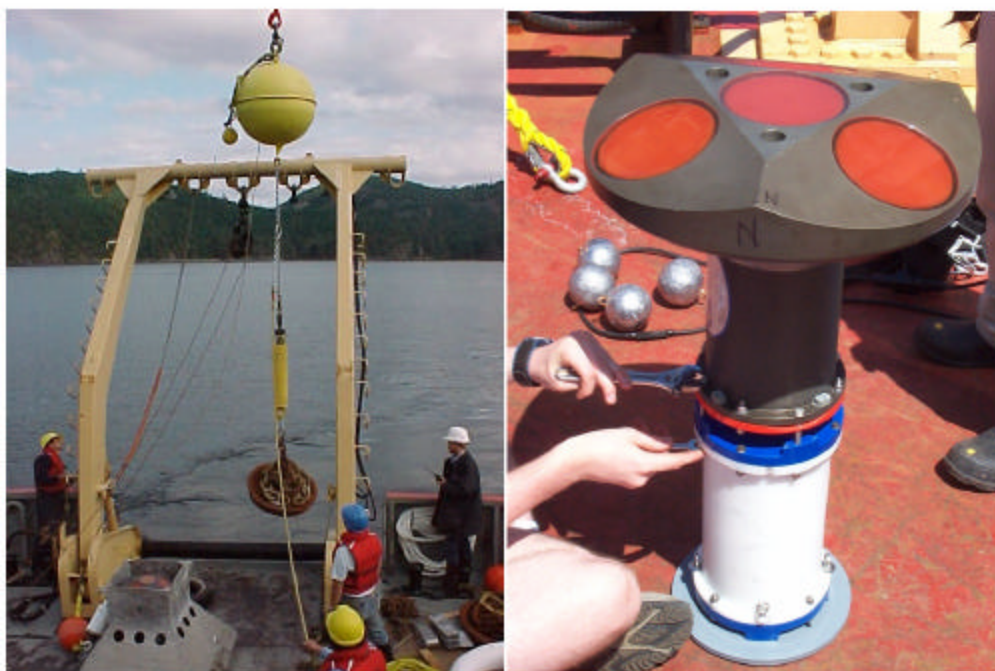


Figure 5. Deployment of the 4-beam Cyclops ADCP in Sansum Narrows in August 2000. The ADCP was coupled to an external battery pack and gimballed in a trawl resistant bottom bracket.

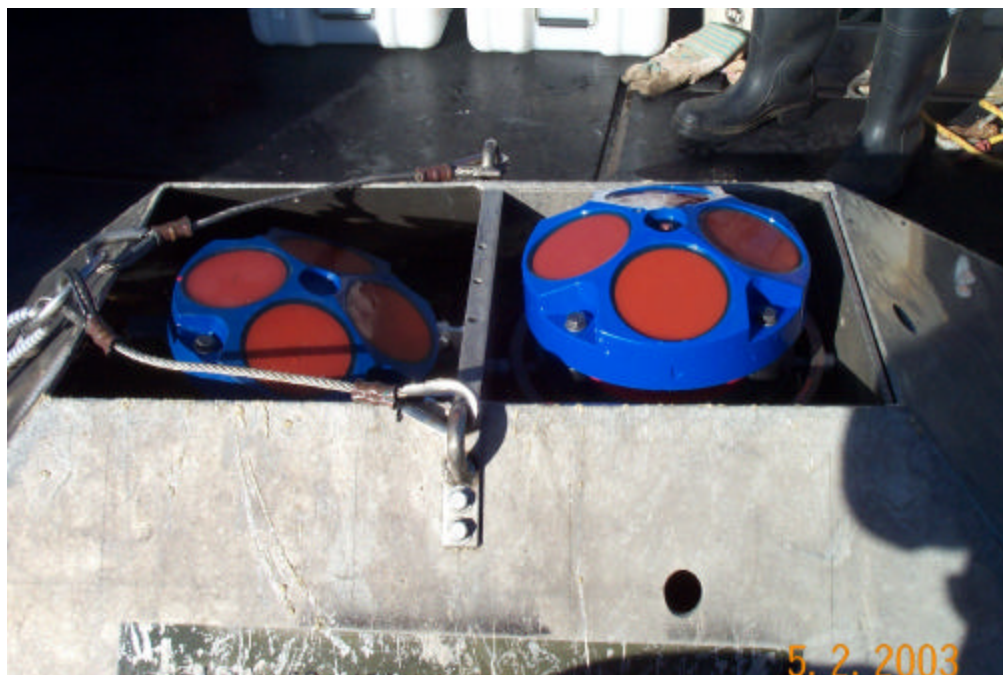


Figure 6. Two 4-beam Janus ADCPs configured in a coupled Master-Slave mode and tilted to produce an effective 5-beam Janus ADCP system.

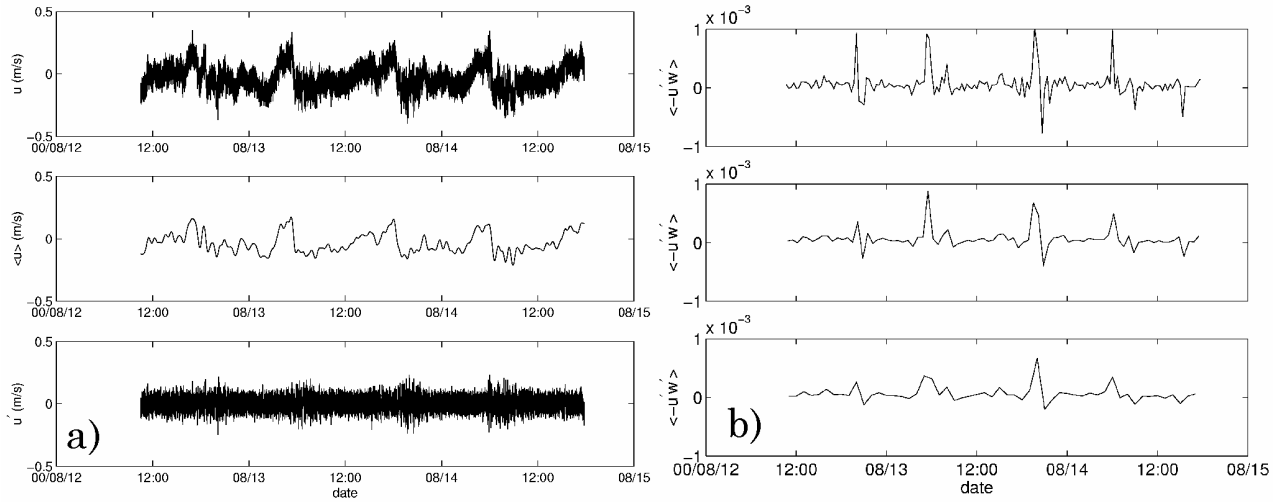


Figure 7. a) The raw, filtered, and residual u velocity record (4-beam Janus, Aug 2000). b) The Reynolds stresses (beam variance method, eq 5.6) calculated over 2, 4, and 6 minute intervals from the residual beam velocities.

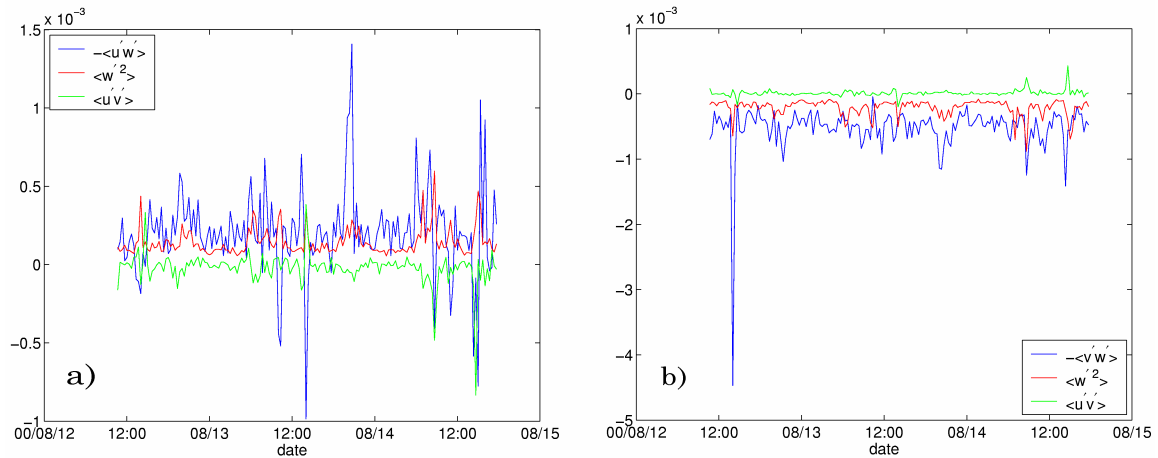


Figure 8. Reynolds stress estimates from a 4-beam Janus (Aug. 2000), including the two bias terms (red and green) associated with non-zero pitch and roll angles. Data are from a depth/height of 60/20 metres.

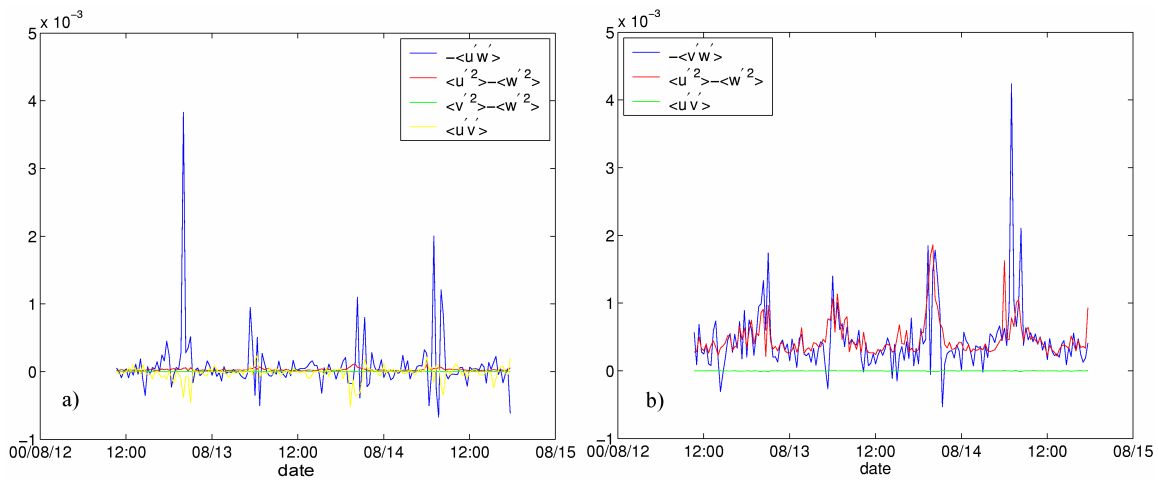


Figure 9. Reynolds stress estimates from a 4-beam Cyclops ADCP (Aug. 2000), including the bias terms (red, green, and yellow) associated with non-zero pitch and roll angles. Data are from a depth/height of 60/20 metres.

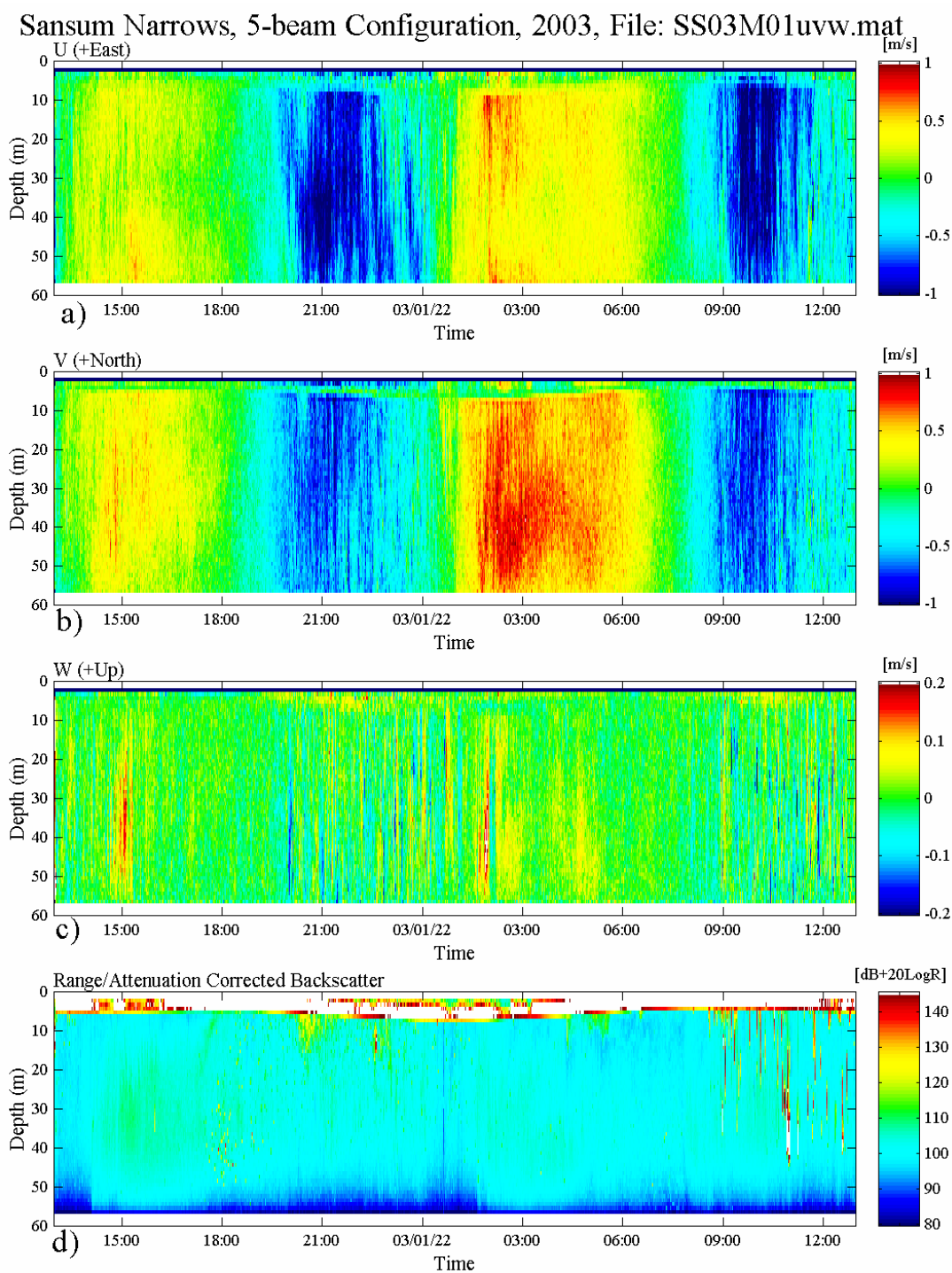


Figure 10. Four-beam Janus velocities a) U, b) V, c) W, and d) backscatter for one day in Sansum Narrows as the Master ADCP in a 5-beam Janus configuration.

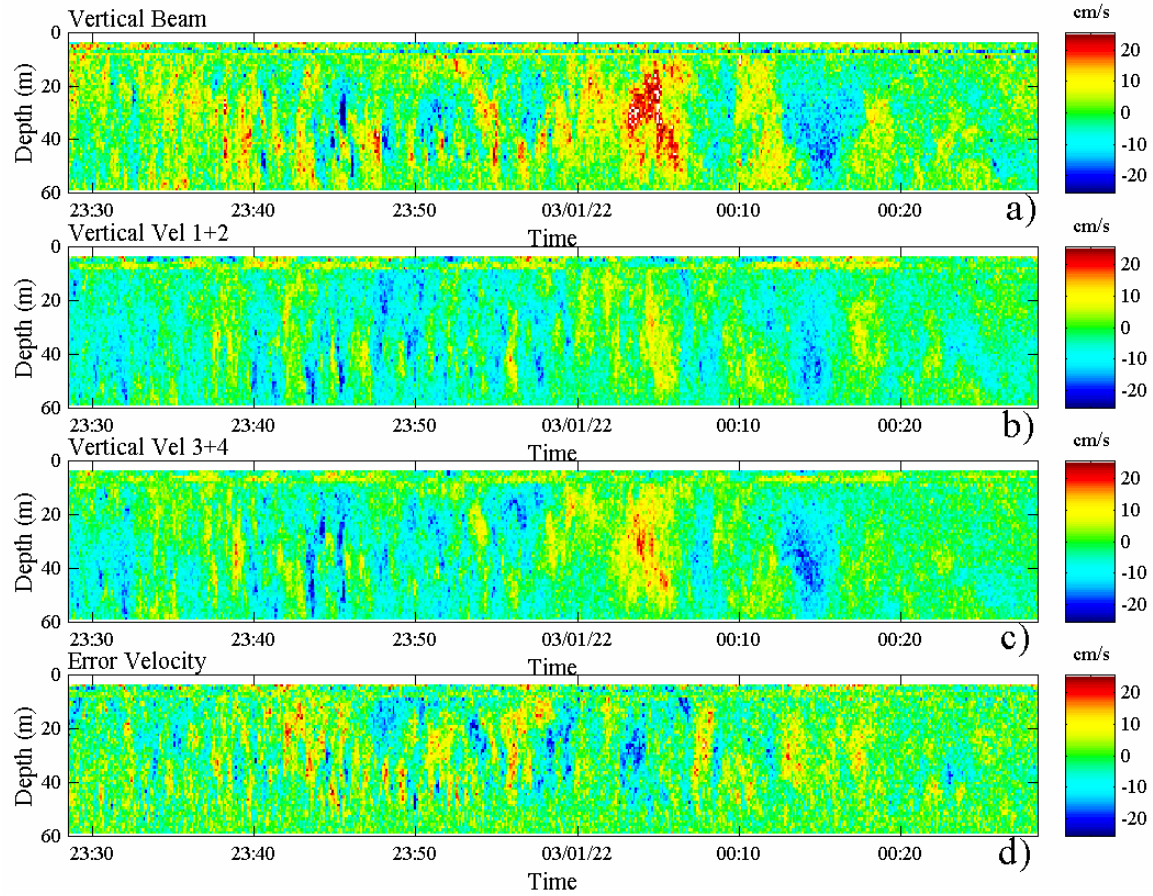


Figure 11. Vertical velocities W , from top to bottom, a) the vertical beam (Slave), b) W_{12} from Master beams 1 & 2, c) W_{34} from Master beams 3 & 4, and d) the Master error velocity.